

Changes in the global hydrological-cycle inferred from ocean salinity

Kieran P. Helm,^{1,2} Nathaniel L. Bindoff,^{1,2,3,4} and John A. Church^{2,3,4}

Received 6 June 2010; revised 21 July 2010; accepted 10 August 2010; published 22 September 2010.

[1] Using global datasets of in situ observations, we calculate salinity changes on ocean-density surfaces between 1970 and 2005. This reveals a global pattern of increased salinities near the upper-ocean salinity-maximum layer (average depth of ~100 m) and decreased salinities near the intermediate salinity minimum (average depth of ~700 m). The salinity changes imply a $3 \pm 2\%$ decrease in precipitation-minus evaporation (P-E) over the mid and low latitude oceans in both hemispheres, a $7 \pm 4\%$ increase in the Northern Hemisphere high latitudes, and a $16 \pm 6\%$ increase in the Southern Ocean since 1970. This pattern of increased precipitation at high latitudes and decreased precipitation in the subtropics is reflected in both land records and in the short satellite records. The quantification of the atmospheric signal of climate change on ocean salinity supports model projections, and extends the growing evidence for an acceleration of the Earth's water cycle. **Citation:** Helm, K. P., N. L. Bindoff, and J. A. Church (2010), Changes in the global hydrological-cycle inferred from ocean salinity, *Geophys. Res. Lett.*, 37, L18701, doi:10.1029/2010GL044222.

1. Introduction

[2] The temperature and salinity properties of surface waters are set by air-sea, ice-sea and land-sea exchange. These properties are carried into the subsurface ocean along surfaces of constant density (isopycnals). Weak diapycnal mixing means that ocean temperature and salinity anomalies are largely preserved as the water is spread along density surfaces into the ocean interior far from their source region [Ledwell et al., 1993]. Consequently, changes in air-sea heat fluxes and precipitation-minus-evaporation in the formation region can be inferred from observed changes of temperature and salinity on constant density surfaces [Bindoff and McDougall, 1994]. These surfaces are thus a more natural reference system than depth coordinates for linking changes in ocean salinity with atmospheric air-sea fluxes. Indeed, by investigating changes along density surfaces, much of the geophysical noise associated with vertical movement of the thermocline caused by ocean eddies and other internal variability can be removed [McDougall, 1987].

[3] Coupled global climate models suggest that the hydrological cycle has intensified over the last 50 years, resulting in

more saline surface waters in the low latitudes, and fresher surface waters in the equatorial region and at higher latitudes [Allen and Ingram, 2002; Held and Soden, 2006; Meehl et al., 2007]. These changes are reflected in the limited land [Zhang et al., 2007] and satellite observations [Wentz et al., 2007]. Changes in ocean salinity on density surfaces along a few repeated trans-ocean sections [Aoki et al., 2005a; Arbic and Owens, 2001; Bindoff and McDougall, 2000; Bryden et al., 2003, 1996; Curry et al., 2003; Johnson and Orsi, 1997; Wong et al., 1999], in a few regions of dense historical data coverage [Curry and Mauritzen, 2005; Stott et al., 2008] and on pressure surfaces [Boyer et al., 2005] are qualitatively consistent with these projected changes.

[4] The IPCC recognise the relationship between the hydrological cycle and ocean salinity in their 2007 report, however it stated that “the data and analyses have been insufficient to identify in detail the origin of these changes” [Bindoff et al., 2007]. Here we address this deficiency by combining the high resolution Argo dataset with historical data in an analysis of salinity changes along layers of a constant density. This dataset provides comprehensive global coverage (Figure 1), while the use of density surfaces reflects the primary pathways in which surface waters are mixed into the ocean interior [Ledwell et al., 1993; McDougall, 1987]. The increase in salinity in the upper thermocline and freshening at the salinity minimum show a consistent pattern across all ocean basins. This supports model projections of a global intensification of the hydrological cycle.

2. Data and Methods

[5] The World Climate Research Programme's World Ocean Circulation Experiment (WOCE) data was used as a baseline (1988–1995), as it is unique in its quality, comprehensiveness and global coverage. To detect historical changes in ocean salinities, approximately 800,000 full-depth temperature and salinity profiles taken between 1940 and 1987 were objectively mapped onto the location of 38,463 profiles taken during the WOCE period (Figure 1). To determine more recent salinity changes, the same technique was used to map approximately 170,000 globally distributed Argo float profiles to the WOCE locations.

[6] The optimal-interpolation mapping technique adopted was based on the same Gaussian correlation function used in previous studies [Bindoff and McDougall, 2000]. The historical and Argo observations surrounding each WOCE observation (x_j, y_j) were weighted by their time (t_i) and location (x_i, y_i)

$$\exp\left(\left(\frac{x_i - x_j}{lon\text{scale}}\right)^2 + \left(\frac{y_i - y_j}{latscale}\right)^2 + \left(\frac{t_i - t_j}{years\text{scale}}\right)^2\right)^{-1} \quad (1)$$

¹Institute of Marine and Antarctic Studies, University of Tasmania, Hobart, Tasmania, Australia.

²Antarctic Climate and Ecosystems Cooperative Research Centre, Sandy Bay, Tasmania, Australia.

³CSIRO Marine and Atmospheric Research, Hobart, Tasmania, Australia.

⁴Wealth From Oceans Flagship, Tasmania, Australia.

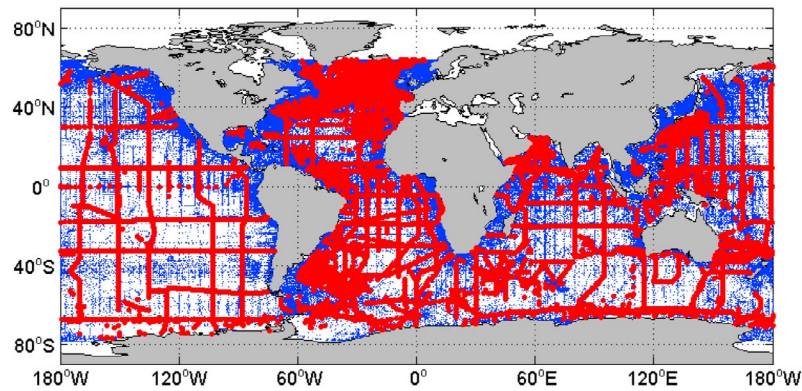


Figure 1. Distribution of temperature and salinity profiles used in this analysis. The 38,463 red points represent profiles taken in the 1988 to 1995 period and come mainly from the World Ocean Circulation Experiment. The 816,193 blue points represent historical profiles taken during the 1940 to 1987 period. The 172,918 Argo profiles (2002 to 2007) are not shown, however are fairly uniform in distribution between 60°S and 64°N. All historical and Argo profiles were mapped to the red points to allow temporal changes in salinity to be determined.

To accommodate varying spatial scales in the ocean an adaptive iterative procedure to determine the length scales was employed, where the latitude and longitude scales were dependent on the residual variance and the independently estimated *a priori* noise.

[7] This method of interpolating 1940–1987 and Argo data to common WOCE locations allowed three periods to be compared: 1940–1987 ($t_j = 1970$), 1988–1995 ($\bar{t} = 1992$), and 2002–2007 ($t_j = 2005$). The sparsity of full depth profiles in the Southern Hemisphere limits the usefulness of determining a more complete time series.

[8] Unlike the more common isobaric analysis, the objective mapping was performed using observations on neutral density surfaces [Jackett and McDougall, 1997]. These surfaces reflect the primary pathways of ocean flow and are referred to as ‘density surfaces’ throughout this manuscript. All uncertainty estimates are provided as a 90% confidence interval.

[9] Ocean profiles in water depth shallower than 1000 m, and observations in the upper 100 m were removed to reduce coastal effects and seasonal variability respectively. In addition we excluded the denser water masses below 1500 m poleward of 60°N and 60°S, where there is insufficient Argo data.

[10] Estimates of P-E were obtained by integrating the salinity change and volume along density surfaces from the outcrop region to the equator in each hemisphere. The assumption was made that there is no change in diapycnal mixing and that all first-order freshwater differences are due to P-E changes. In the near-equatorial regions P-E changes were unable to be resolved using this method.

[11] The estimates of surface freshwater flux from observations were then compared with the mean change in P-E from ten IPCC-class coupled climate models determined from ten-year averages centered on 1970 and 2000. The coupled models are: CGCM3.1(T47) (Canada), CSIRO-Mk3.0 (Australia), GFDL-CM2.1 (USA), GISS-AOM (USA), INM-CM3.0 (Russia), IPSL-CM4 (France), MIROC3.2 (Medres) (Japan), MRICGCM2.3.2 (Japan), PCM (USA), and UKMO-HadCM3 (UK). Details of IPCC model output

can be found in the work of Randall *et al.* [2007] and PCMDI (<http://www.pcmdi.llnl.gov/>).

3. Changes in Ocean Salinity

[12] Our analysis shows temperature and salinity increases along density surfaces in the upper thermocline virtually throughout the world ocean (Figures 2a and 3c). When looking along density surfaces, an increase in salinity above the shallow salinity maximum may be a result of surface warming and/or salinity increases. At the upper-ocean maximum in salinity ($\sim 24.8 \text{ kg m}^{-3}$ density surface) however, the globally averaged increase of 0.11 ± 0.08 pss (practical salinity scale) can only be explained by a change in salinity. This indicates (at least to first order) a decrease in precipitation-minus-evaporation in the low-latitude formation regions of these water masses [Bindoff and McDougall, 1994]. Warming and salinity increases on density surfaces in the upper thermocline previously have been observed along individual sections, however here the signal is shown to be coherent across all oceans.

[13] From 1970 to 2005, the Atlantic Ocean upper thermocline waters were observed to increase in salinity by 0.17 ± 0.09 pss. This increase occurred at similar rates for the ~ 1970 to 1992 and ~ 1992 to 2005 periods (Table 1). In the Indian Ocean the majority of the total 0.09 ± 0.06 pss salinity increase occurs before 1992. In the Pacific Ocean, there is an average increase of 0.09 ± 0.07 pss (~ 1970 to 2005). This is reflected in a spatially coherent pattern, with $\sim 80\%$ of grid cells showing an increase in salinity. The interpolation method used smoothes out inter-annual signals, thus reducing the effects of aliasing from the El Niño Southern Oscillation in the equatorial Pacific Ocean. The salinity maximum layer does not outcrop poleward of 30° in either hemisphere.

[14] The waters of the main thermocline (below 26.4 kg m^{-3} , 200–300 m) to the salinity minimum Intermediate Waters (~ 1000 m depth) have freshened and cooled on density surfaces across most of the globe (Figure 3c). For Intermediate Waters in the density range $26.8\text{--}27.2 \text{ kg m}^{-3}$ (300–1000 m), this freshening at the salinity minimum is almost certainly in response to decreased salinity in the surface source regions.

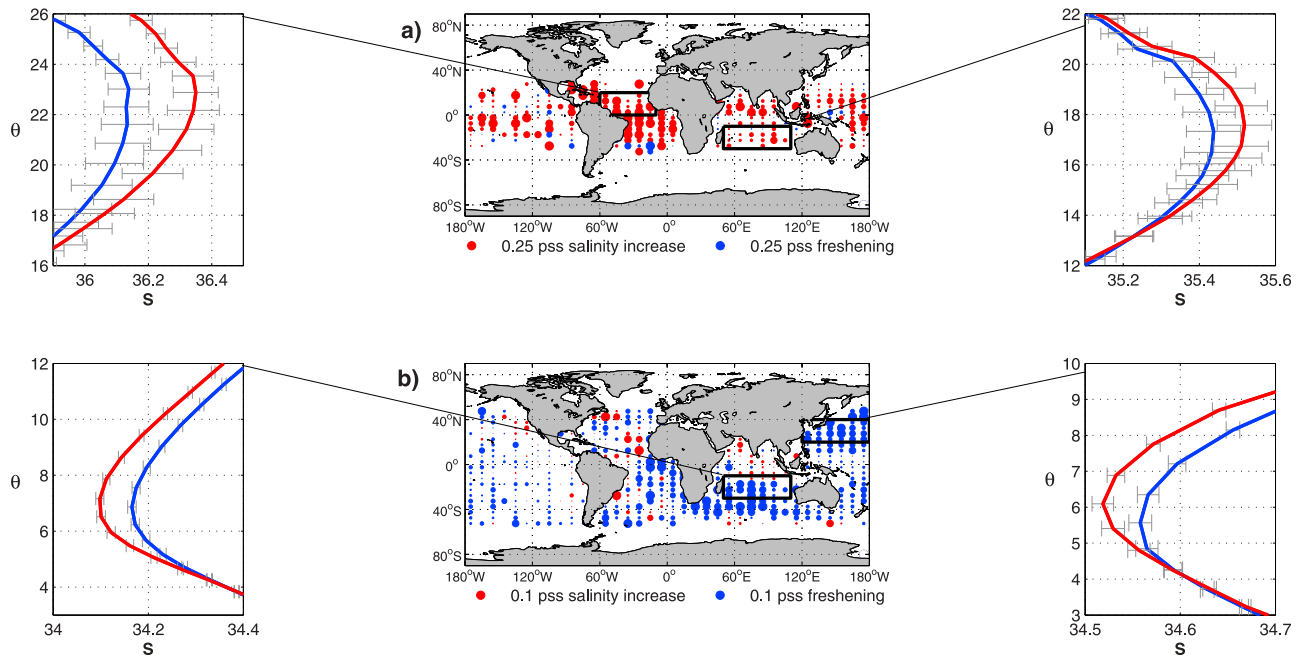


Figure 2. Salinity changes of key water masses within the ocean (1970 to 2005). Changes are shown along (a) the salinity maximum density surface and (b) the salinity minimum density surface. Each dot represents the average salinity change inside the $5^\circ \times 10^\circ$ grid cell. The top-left and top-right boxes show the average temperature–salinity plot for the corresponding boxed regions and are centered on the salinity maximum (~ 100 m). The bottom-left and bottom-right boxes show average changes at the salinity minimum (~ 600 – 1000 m). The blue line represents the average during the 1940 to 1987 period (weighted to 1970) and the red line represents the 2002 to 2007 period (weighted to 2005). The horizontal error bars on the temperature–salinity curves show one standard deviation of the salinity observations.

The largest decreases (Figure 2b) are in the South Indian and North Pacific subtropical gyres (latitudes 20° to 40° N and S), and in the eastern tropical Atlantic Ocean. Although the North Atlantic does not have a well defined salinity minimum, recently ventilated intermediate depth waters in this ocean show the same coherent pattern of freshening and cooling on density surfaces as the rest of the global ocean. There are smaller changes in the North Indian Ocean, where land and the equatorial region act to isolate this gyre from the rest of the global circulation.

[15] Antarctic Intermediate Water (AAIW), distributed throughout all of the Southern Hemisphere sub-tropical gyres by the Antarctic Circumpolar Current, has freshened and cooled on density surfaces between 1970 and 2005 (Figure 2b). In the global zonally averaged vertical section (Figure 3c) the freshening in the subtropical gyres on the 26.8 – 27.0 kg m^{-3} (~ 400 – 700 m^3) is clearly visible. This AAIW with modified properties reaches the equatorial regions via low-latitude western boundary currents, particularly in the South-West Pacific and South-West Indian Oceans where large changes are observed that are consistent with this circulation pathway (Figure 2b). Changes in Sub-Antarctic Mode Water (SAMW) in the Southern Ocean also show a global-scale pattern of cooling and freshening on density surfaces (similar to Figures 2b and 3c: 20°S – 40°S). These observations extend the earlier regional results [Curry *et al.*, 2003; Wong *et al.*, 1999] to all of the Southern Hemisphere Oceans.

[16] In the Atlantic Ocean between 50°S and 10°S , the freshening in AAIW is centered on the 27.2 kg m^{-3} neutral density surface. In this region the surface had an average

salinity decrease of 0.04 ± 0.04 pss between 1970 and 2005, with the majority of change occurring between 1970 and 1992. North Pacific Intermediate Water (~ 26.8 kg m^{-3} and 600 m) shows a broad pattern of freshening between 20°N and 35°N with an average decrease of 0.07 ± 0.02 pss between 1970 and 2005. This freshening appears to strengthen over the last decade with an increase in the rate of freshening from 1.2 ± 1.1 pss yr^{-1} (1970 to 1992) to 2.8 ± 1.6 pss yr^{-1} (1992 to 2005). Poleward of 40°N , Atlantic Ocean waters in the depth range 300 – 1500 m were initially freshening (1970 to 1992) in density range 26.8 – 27.2 kg m^{-3} but are now more saline on density surfaces (1970 to 2005) (Figure 3c). These changes largely originate from Labrador Sea Water where decadal oscillations in salinity are well documented [Bindoff *et al.*, 2007; Yashayaev, 2007].

[17] In the low and mid latitudes of both hemispheres there is little evidence of change in water mass properties below 1500 m between 1970 and 1992 far from their source regions (not shown). Close to the source regions of the deep waters there is evidence of salinity variations in North Atlantic Deep Water and of freshening in Antarctic Bottom Water. These variations tend to be associated with ice melt [Aoki *et al.*, 2005b; Bindoff *et al.*, 2007; Rintoul, 2007; Yashayaev, 2007]. The majority of modern Argo floats do not profile below 2000 m, thus precluding a longer term analysis of deep water changes.

4. Inferred Changes in the Global Hydrological Cycle

[18] Changes in the hydrological cycle can be inferred from observed salinity changes. We achieve this by integrating the

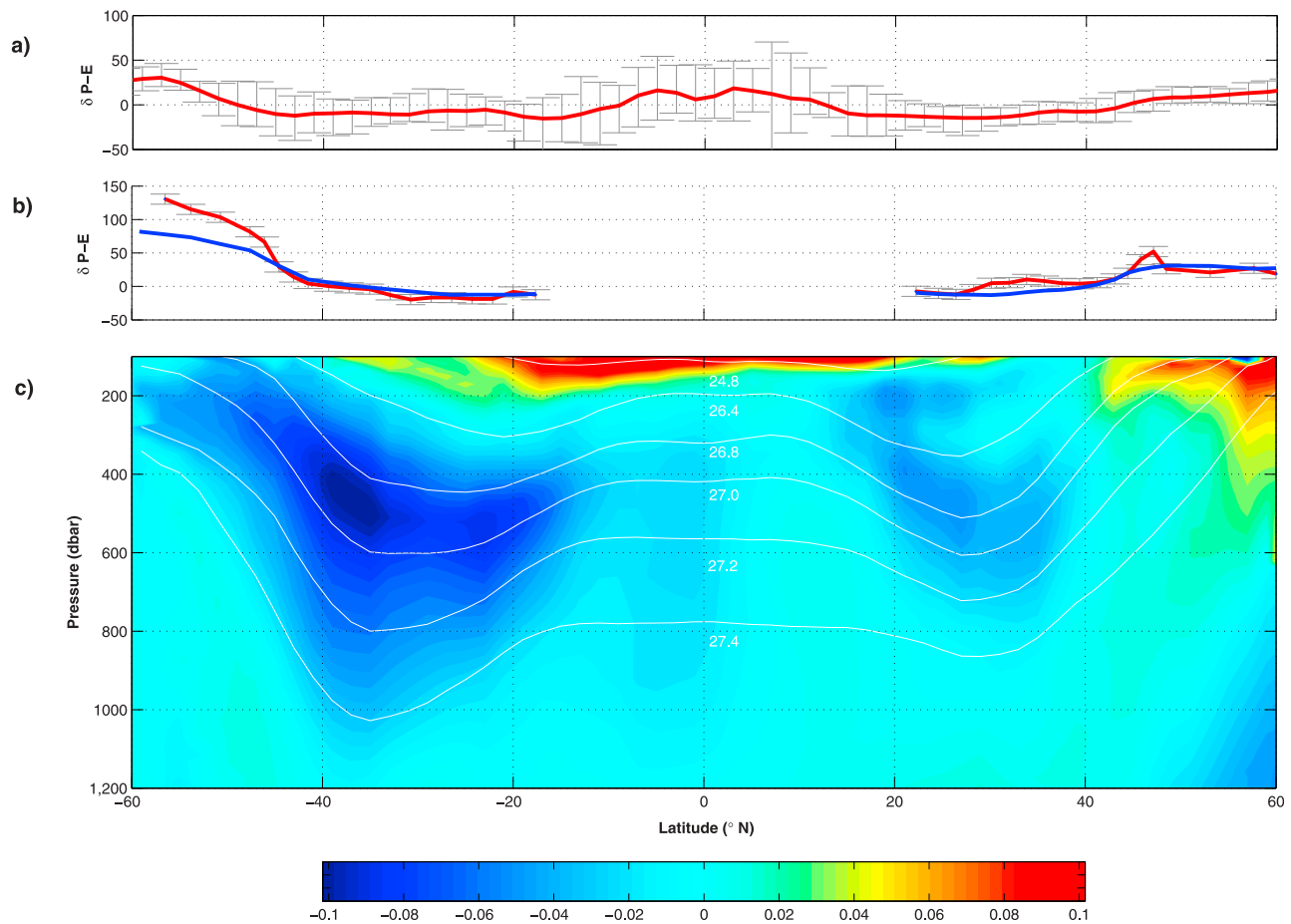


Figure 3. Zonally averaged changes in salinity and inferred changes in precipitation-minus-evaporation (P-E). (a) Projected change in P-E (mm yr^{-1}) from ten IPCC-class models for the period 1970 to 2000. The red line is an average change across each 2° latitude band (x-axis), while the error bars show the 10% and 90% percentile range. P-E changes over land are included in this analysis and are assumed to be transferred immediately to the oceans as runoff. (b) Inferred difference in P-E (mm yr^{-1}), using salinity observations, at the ocean surface of each isopycnal layer (~ 1970 to 2005). The red line illustrates the inferred P-E difference between 1970 and 2005, while the blue line illustrates the inferred P-E difference between 1970 and 1992. Error bars are shown to two standard deviations. (c) Zonally averaged salinity difference along density layers, where blue represents freshening and red represents an increase in salinity.

salinity change and volume of density layers, from the equator poleward to the intersection of these layers with the ocean surface. The estimated surface freshwater flux from this approach reveals a striking pattern of the strong addition of freshwater south of 45°S (up to $100 \pm 15 \text{ mm yr}^{-1}$ near Antarctica), while north of 45°N there was a smaller addition of freshwater. Statistically significant decreases in the freshwater input were observed in the mid-latitudes in both hemispheres (Figure 3b). Based on model P-E climatologies this observed freshwater flux change represents a $16 \pm 6\%$ increase in the Southern Ocean, a $7 \pm 4\%$ increase in the Northern Hemisphere high latitudes, and a decrease of $3 \pm 2\%$ in the subtropical gyres of both hemispheres (~ 1970 to 2005).

[19] The increase in freshwater flux in the Northern Hemisphere occurs in spite of the observed increase in the zonally averaged salinity poleward of 40°N (Figure 3c). Here the strongest salinity increases occur in the upper 500 m and are not large enough to counteract the freshening observed south of 40°N to the equator in the $26.8\text{--}27.4 \text{ kg m}^{-3}$ density range. This therefore leads to a net positive surface freshwater flux (Figure 3b). Such salinity fluctuations in the subpolar

North Atlantic are well documented and have been at least partially attributed to variability in ice melt, ocean circulation, and river runoff in the Labrador Sea [Bindoff *et al.*, 2007; Yashayaev, 2007].

[20] Examining output from ten IPCC-class coupled ocean-atmosphere general circulation models we see a similar pattern of P-E increases in the high-latitudes and P-E decreases in the subtropical gyres (Figure 3a, red line). Despite significant inter-model variability over the period

Table 1. Average Change in Salinity at the Upper Thermocline Salinity Maximum ($\sim 24.8 \text{ kg m}^{-3}$ and 100 m) by Ocean^a

Ocean	Salinity Change 1970 to 2005	Annual Rate of Salinity Change	
		1970 to 1992	1992 to 2005
Atlantic	0.17 ± 0.09	0.005 ± 0.004	0.006 ± 0.008
Indian	0.09 ± 0.06	0.004 ± 0.004	0.003 ± 0.007
Pacific	0.09 ± 0.07	0.001 ± 0.004	0.005 ± 0.006
Global	0.11 ± 0.08	0.003 ± 0.004	0.004 ± 0.007

^aThe salinity change from ~ 1970 to 2005 is expressed in pss, while the rates of salinity change are given as pss yr^{-1} .

1970 to 2000, an average of the models shows P-E decreases in the low latitudes of a similar magnitude to the observations ($\sim 20 \text{ mm yr}^{-1}$). In the high latitudes of the Northern Hemisphere ($\sim 60^\circ\text{N}$) the magnitude of the projected P-E increases are similar to those observed ($\sim 30 \text{ mm yr}^{-1}$).

[21] In the Southern Hemisphere high latitudes the estimated freshwater flux is larger than the simulated P-E changes, although IPCC coupled models typically do not include freshwater sources from Antarctic ice sheets and ice shelves. It is tantalising to speculate that these differences in magnitude in the Southern Ocean could be due to changes in the melt of floating ice shelves (as has been suggested in freshening Antarctic Bottom Water [Bindoff et al., 2007]. Our estimates indicate that less than 0.5% of the floating shelves around Antarctica would need to have melted between 1970 and 2005 to make up this difference between inferred freshwater flux and simulations.

5. Conclusion

[22] Analyzing ocean salinity changes along density surfaces reveals a pattern of change that is strikingly coherent on a global scale ($\sim 1970\text{--}2005$). We find increased salinities near the upper-ocean salinity-maximum layer and decreased salinities near the intermediate salinity minimum. The density layers near salinity-maximum outcrop into the mixed layer in the subtropics ($10^\circ\text{--}35^\circ$) where evaporation dominates precipitation. Conversely, the comparatively fresh Intermediate Water outcrops in the mid to high latitudes where precipitation dominates evaporation.

[23] While regional variability may occur (El Niño, North Atlantic Oscillation etc), the global strength of these observed salinity changes and the coherence of these patterns between these two separate time periods suggests that there are overriding changes in the global hydrological cycle. The strong correspondence of the estimated surface freshwater fluxes for the 1970 to 2005 period with the simulated patterns of P-E changes in the atmosphere over the same period, lends strong support for a conclusion that the global hydrological cycle has accelerated.

[24] **Acknowledgments.** This paper is a contribution to the CSIRO Climate Change Research Program and was supported by the Australian Governments Cooperative Research Centres Programme through the Antarctic Climate and Ecosystems Cooperative Research Centre.

References

- Allen, M. R., and W. J. Ingram (2002), Constraints on future changes in climate and the hydrologic cycle, *Nature*, 419(6903), 224–232, doi:10.1038/nature01092.
- Aoki, S., N. L. Bindoff, and J. A. Church (2005a), Interdecadal water mass changes in the Southern Ocean between 30°E and 160°E , *Geophys. Res. Lett.*, 32, L07607, doi:10.1029/2004GL022220.
- Aoki, S., S. R. Rintoul, S. Ushio, S. Watanabe, and N. L. Bindoff (2005b), Freshening of the Adelic Land Bottom Water near 140°E , *Geophys. Res. Lett.*, 32, L23601, doi:10.1029/2005GL024246.
- Arbic, B. K., and W. B. Owens (2001), Climatic warming of Atlantic intermediate waters, *J. Clim.*, 14(20), 4091–4108, doi:10.1175/1520-0442(2001)014<4091:CWOAIW>2.0.CO;2.
- Bindoff, N. L., and T. J. McDougall (1994), Diagnosing climate-change and ocean ventilation using hydrographic data, *J. Phys. Oceanogr.*, 24(6),

- 1137–1152, doi:10.1175/1520-0485(1994)024<1137:DCCAOV>2.0.CO;2.
- Bindoff, N. L., and T. J. McDougall (2000), Decadal changes along an Indian ocean section at 32°S and their interpretation, *J. Phys. Oceanogr.*, 30(6), 1207–1222, doi:10.1175/1520-0485(2000)030<1207:DCAAIO>2.0.CO;2.
- Bindoff, N. L., et al. (2007), Observations: Oceanic climate change and sea level, in *Climate Change 2007: The Physical Science Basis: Contribution of Working Group I to the Fourth Assessment Report of the Intergovernmental Panel on Climate Change*, edited by S. Solomon et al., pp. 385–432, Cambridge Univ. Press, New York.
- Boyer, T. P., S. Levitus, J. I. Antonov, R. A. Locarnini, and H. E. Garcia (2005), Linear trends in salinity for the World Ocean, 1955–1998, *Geophys. Res. Lett.*, 32, L01604, doi:10.1029/2004GL021791.
- Bryden, H. L., M. J. Griffiths, A. M. Lavin, R. C. Millard, G. Parrilla, and W. M. Smethie (1996), Decadal changes in water mass characteristics at 24°N in the subtropical North Atlantic ocean, *J. Clim.*, 9(12), 3162–3186, doi:10.1175/1520-0442(1996)009<3162:DCIWMC>2.0.CO;2.
- Bryden, H. L., E. L. McDonagh, and B. A. King (2003), Changes in ocean water mass properties: Oscillations or trends?, *Science*, 300(5628), 2086–2088, doi:10.1126/science.1083980.
- Curry, R., and C. Mauritzen (2005), Dilution of the northern North Atlantic Ocean in recent decades, *Science*, 308, 1772–1774.
- Curry, R., B. Dickson, and I. Yashayaev (2003), A change in the freshwater balance of the Atlantic Ocean over the past four decades, *Nature*, 426(6968), 826–829, doi:10.1038/nature02206.
- Held, I. M., and B. J. Soden (2006), Robust responses of the hydrological cycle to global warming, *J. Clim.*, 19(21), 5686–5699, doi:10.1175/JCLI3990.1.
- Jackett, D. R., and T. J. McDougall (1997), A neutral density variable for the world's oceans, *J. Phys. Oceanogr.*, 27(2), 237–263, doi:10.1175/1520-0485(1997)027<0237:ANDVFT>2.0.CO;2.
- Johnson, G. C., and A. H. Orsi (1997), Southwest Pacific Ocean water-mass changes between 1968/69 and 1990/91, *J. Clim.*, 10(2), 306–316, doi:10.1175/1520-0442(1997)010<0306:SPOWMC>2.0.CO;2.
- Ledwell, J. R., A. J. Watson, and C. S. Law (1993), Evidence for slow mixing across the pycnocline from an open-ocean tracer-release experiment, *Nature*, 364(6439), 701–703, doi:10.1038/364701a0.
- McDougall, T. J. (1987), Neutral surfaces, *J. Phys. Oceanogr.*, 17(11), 1950–1964, doi:10.1175/1520-0485(1987)017<1950:NS>2.0.CO;2.
- Meehl, G. A., et al. (2007), Global climate projections, in *Climate Change 2007: The Physical Science Basis: Contribution of Working Group I to the Fourth Assessment Report of the Intergovernmental Panel on Climate Change*, edited by S. Solomon et al., pp. 747–846, Cambridge Univ. Press, New York.
- Randall, D. A., et al. (2007), Climate models and their evaluation, in *Climate Change 2007: The Physical Science Basis: Contribution of Working Group I to the Fourth Assessment Report of the Intergovernmental Panel on Climate Change*, edited by S. Solomon et al., pp. 589–662, Cambridge Univ. Press, New York.
- Rintoul, S. R. (2007), Rapid freshening of Antarctic Bottom Water formed in the Indian and Pacific oceans, *Geophys. Res. Lett.*, 34, L06606, doi:10.1029/2006GL028550.
- Stott, P. A., R. T. Sutton, and D. M. Smith (2008), Detection and attribution of Atlantic salinity changes, *Geophys. Res. Lett.*, 35, L21702, doi:10.1029/2008GL035874.
- Wentz, F. J., L. Ricciardulli, K. Hilburn, and C. Mears (2007), How much more rain will global warming bring?, *Science*, 317(5835), 233–235, doi:10.1126/science.1140746.
- Wong, A. P. S., N. L. Bindoff, and J. A. Church (1999), Large-scale freshening of intermediate waters in the Pacific and Indian oceans, *Nature*, 400(6743), 440–443, doi:10.1038/22733.
- Yashayaev, I. (2007), Changing freshwater content: Insights from the subpolar North Atlantic and new oceanographic challenges, *Prog. Oceanogr.*, 73(3–4), 203–209, doi:10.1016/j.pocan.2007.04.014.
- Zhang, X. B., F. W. Zwiers, G. C. Hegerl, F. H. Lambert, N. P. Gillett, S. Solomon, P. A. Stott, and T. Nozawa (2007), Detection of human influence on twentieth-century precipitation trends, *Nature*, 448(7152), 461–465, doi:10.1038/nature06025.

N. L. Bindoff and K. P. Helm, Institute of Marine and Antarctic Studies, University of Tasmania, Hobart, Tas 7001, Australia. (n.bindoff@utas.edu.au)
J. A. Church, CSIRO Marine and Atmospheric Research, Hobart, 7001 Tas, Australia.